Precise targeting of miRNA sites restores CFTR activity in CF bronchial epithelial cells.

AUTHOR(S)

Chiara De Santi, Elena Fernandez Fernandez, Rachel Gaul, Sebastian Vencken, Arlene Glasgow, Irene Oglesby, Killian Hurley, Finn Hawkins, Nilay Mitash, Fangping Mu, Rana Raoof, David Henshall, Meritxell B. Cutrona, Jeremy C. Simpson, Brian Harvey, Barry Linnane, Paul McNally, Sally-Ann Cryan, Ronan MacLoughlin, Agnieszka Swiatecka-Urban, Catherine Greene

Precise targeting of miRNA sites restores CFTR activity in CF bronchial epithelial cells

Chiara De Santi[1,*], Elena Fernández Fernández[1], Rachel Gaul[2], Sebastian Vencken[1], Arlene Glasgow[1], Irene K. Oglesby[3], Killian Hurley[3], Finn Hawkins[4], Nilay Mitash[5], Fangping Mu[6], R Raoof[7], D Henshall[7], Meritxell B. Cutrona[8], Jeremy C. Simpson[8], Brian J. Harvey[9], Barry Linnane[10], Paul McNally[11], Sally Ann Cryan[2], Ronan MacLoughlin[12], Agnieszka Swiatecka-Urban[5] and Catherine M. Greene[1]

[1] Department of Clinical Microbiology, Royal College of Surgeons in Ireland, Dublin, Ireland

[2] School of Pharmacy and Tissue Engineering Research Group, Royal College of Surgeons in Ireland, Dublin, Ireland

[3] Department of Medicine, Royal College of Surgeons in Ireland, Dublin, Ireland

[4] Center for Regenerative Medicine, Boston University and Boston Medical Center, Boston, MA 02118, USA and The Pulmonary Center and Department of Medicine, Boston University School of Medicine, Boston, MA 02118, USA

[5] Department of Pediatrics, University of Pittsburgh School of Medicine, Pittsburgh, USA

[6] Center for Research Computing, University of Pittsburgh, Pittsburgh, USA

[7] Department of Physiology and Medical Physics, Royal College of Surgeons in Ireland, Dublin, Ireland

[8] School of Biology and Environmental Science, Conway Institute of Biomolecular and Biomedical Research, University College Dublin, Dublin, Ireland

[9] Department of Molecular Medicine, Royal College of Surgeons in Ireland, Dublin, Ireland

[10] University Hospital Limerick, Limerick, Ireland

[11] Department of Pediatrics, Royal College of Surgeons in Ireland, Dublin, Ireland and National Children's Research Centre, Children's Health Ireland at Crumlin, Dublin, Ireland

[12] Aerogen Limited, Galway, Ireland

* Correspondence should be addressed to C.D.S. Tel: +35314028519; Fax: +35318093808; Email: chiaradesanti@rcsi.ie

Short title: miRNA inhibition as tool to restore CFTR activity

ABSTRACT

MicroRNAs that are overexpressed in cystic fibrosis (CF) bronchial epithelial cells (BEC) negatively regulate *CFTR* and nullify the beneficial effects of CFTR modulators. We hypothesized that it is possible to reverse microRNA-mediated inhibition of CFTR using CFTR-specific target site blockers (TSBs) and to develop a drug-device combination inhalation therapy for CF. Lead microRNA expression was quantified in a series of human CF and non-CF samples and *in vitro* models. A panel of *CFTR* 3'untranslated region-specific locked nucleic acid antisense oligonucleotide TSBs was assessed for their ability to increase CFTR expression. Their effects on CFTR activity alone or in combination with CFTR modulators were measured in CF BEC models. TSBs encapsulation in poly-lactic-co-glycolic acid (PLGA) nanoparticles was assessed as a proof of principle of delivery into CF BECs. TSBs targeting the *CFTR* 3'UTR 298-305:miR-145-5p or 166-173:miR-223-3p sites increased CFTR expression and anion channel activity, and enhanced the effects of Ivacaftor/Lumacaftor or Ivacaftor/Tezacaftor in CF BECs. Respirable PLGA-TSB nanoparticles promoted CFTR expression in primary BECs and retained desirable biophysical characteristics following nebulization. Alone or in combination with CFTR modulators, aerosolized CFTR-targeting TSBs encapsulated in PLGA nanoparticles could represent a promising drug-device combination therapy for the treatment for CFTR dysfunction in the lung.

INTRODUCTION

Cystic Fibrosis (CF) is caused by mutation of the Cystic Fibrosis Transmembrane conductance Regulator (*CFTR*) gene. This affects CFTR protein synthesis, folding, trafficking or function.[1,2] *CFTR* encodes a channel that mediates chloride and other anion transport across the apical membrane of epithelial cells. In the lungs, absent or dysfunctional CFTR leads to depletion of the airway surface liquid and mucus dehydration, resulting in impaired mucociliary clearance, chronic infection and inflammation. p.Phe508del is the most common CF-causing mutation worldwide.

We and others have shown that *CFTR* is post-transcriptionally regulated by microRNAs (reviewed in Glasgow *et al*.[3]); the lead miRNAs that have been experimentally validated as regulators of wild type and/or p.Phe508del human *CFTR* are miR-101-3p, miR-145-5p, miR-223p, miR-494-3p and miR-509-3p. Two studies have demonstrated that antagomir- or peptide nucleic acid (PNA)-based inhibitors of miR-145-5p can enhance CFTR expression and/or function in CF bronchial epithelial cells (BECs),[4,5] and another demonstrated PNA-mediated inhibition of miR-509-3p.[6] However, these strategies whilst effective *in vitro*, could have undesired off-target effects on other miR-145-5p or miR-509-3p-regulated genes, as well as causing co-inhibition of other miRNAs.[7]

Target site blockers (TSBs) are locked-nucleic acid antisense oligonucleotides that specifically compete with miRNAs for the binding to individual miRNA recognition elements (MREs) of a target mRNA, hence preventing them from gaining access to those sites. A TSB targeting the miR-9 MRE in Anoctamin 1 (ANO1/TMEM16A) increases ANO1-mediated chloride efflux and mucociliary clearance in CF models.[8] Here we designed a set of CFTR-specific TSBs and assessed their activity as effective blockers of miRNA-mediated inhibition of CFTR. We quantified their effects on CFTR expression and activity in a variety of *in vitro* and *ex vivo* human CF BEC models, alone or in combination with two currently available CFTR therapies, Ivacaftor/ Lumacaftor and Ivacaftor/ Tezacaftor.

Ivacaftor is a CFTR potentiator that increases the open channel probability of CFTR.[9] Lumacaftor is a CFTR corrector that improves intracellular trafficking of misfolded CFTR to the apical surface of the cells.[10] Together they are authorised for the treatment of p.Phe508del/p.Phe508del in CF children >2 years. Tezacaftor, another CFTR corrector, when used in combination with Ivacaftor in p.Phe508del homozygotes or heterozygotes with a residual function CFTR allele, can deliver similar clinical benefits.[11,12] The proinflammatory CF lung milieu can increase expression of miRNAs that regulate CFTR[2,13] and, as has been

shown for miR-145-5p, can nullify correction by Ivacaftor/Lumacaftor.[4] Whether TSBs that target specific miRNA binding sites within the *CFTR* 3'UTR can enhance Ivacaftor/Lumacaftor or Ivacaftor/Tezacaftor correction of CFTR has not been tested.

An ideal therapeutic to treat the pulmonary manifestations of CF would be delivered locally to the lung. Therefore, we encapsulated TSBs within poly-lactic-co-glycolic acid (PLGA) nanoparticles and assessed their toxicity, function and delivery to CF BECs. Importantly, the PLGA-TSB nanoparticles were also coupled with a nebulizer that can generate stable and respirable aerosols, capable of targeted delivery throughout the lung,[14,15] to demonstrate how such a drug-device combination might be translated to the clinic.

RESULTS

All studies were performed using non-CF or p.Phe508del/p.Phe508del cells unless otherwise stated.

Lead miRNA expression in CF BEC lines, primary cells and bronchial brushings

Endogenous levels of the lead miRNAs experimentally validated to regulate CFTR (miR-101-3p, miR-145-5p, miR-223-3p, miR-494-3p, and miR-509-3p) were measured in 16HBE14o$^-$/CFBE41o$^-$ and Nuli-1/Cufi-1. Basally all miRNAs except miR-101-3p were increased, some significantly, in CFBE41o$^-$ vs. 16HBE14o$^-$ (Figure 1A), and all except miR-494-3p were increased in Cufi vs. Nuli and also in adult primary CF vs. non-CF cells as measured by miRNA TaqMan assay (Figure 1B,C). miR-223-3p and miR-509-3p were significantly increased in ALI culture of CFBE41o$^-$ cells stably transfected with Phe508del versus wild-type CFTR as measured by RNA sequencing (Figure 1D).

Lead miRNA levels in two miRNA profiling datasets were quantified. In n=6 each CF and non-CF BECs from children, miR-145-5p and miR-223-3p were increased in CF (7.4 fold, P=0.028 and 4.1 fold, P=0.04), miR-101-3p showed no difference, and miR-494-3p/miR-509-3p were not available on the platform/not detectable. In the original profiling describing increased miR-145/miR-223/miR-494 (which did not delineate between -3p or -5p miRNAs) in p.Phe508del or p.Gly551Asp *CFTR* homozygous or heterozygous bronchial brushings,[16] miR-101 was increased in two of five CF samples, and miR-509-3p was not available in the platform. Overall, the lead miRNAs are detectable at variably increased levels in all CF BECs analysed by different methods. As no single miRNA can be identified as being unique, an inhibition strategy to individually target each of the lead miRNAs was undertaken.

TSB4 and TSB6 increase endogenous CFTR protein levels in CF BECs

In silico predictions using PITA identified all potential MREs for the lead miRNAs in the *CFTR* 3'UTR: miR-101-3p x 5 sites, miR-145-5p x 8 sites, miR-223-3p x 9 sites, miR-494-3p x 6 sites, and miR-509-3p x 3 sites. From this list, nine sites were selected against which target site blockers were designed with an arbitrary ΔΔG cut-off of from -13.46 to -6.03, and the miR-101-3p site at position 1506 (with a ΔΔG of -2.91) (Figure 2A,B and Supplementary Table 1). The efficacy of the TSBs at increasing *CFTR* 3'UTR luciferase expression in CFBE41o$^-$ cells was screened. Luciferase was significantly increased after transfection with TSB4, TSB6, TSB7 and TSB8 vs. NC TSB (Figure 2C).

The effects of TSB4/6/7/8 on endogenous CFTR protein levels were quantified and each had a positive effect. In particular, TSB4 and TSB6 significantly increased unglycosylated band A and/or core glycosylated band B CFTR protein levels in CFBE41o$^-$ (P=0.0077 and P=0.0041) and Cufi-1 (P=0.0026 and P=0.0014) cells compared to NC TSB (Figure 3, Supplementary Fig. 1). These cells are Phe508del and therefore do not express a fully glycosylated mature CFTR band C of 170-220kDa[17] which would be an indicator of CFTR folding and maturation, although there is a faint unidentified high molecular weight band (>198kDa, open triangle) which may reflect this.

Subsequent studies focussed on TSB4 and TSB6. To confirm these TSBs were specific for CFTR, site-specific mutagenesis of the miR-223-3p MRE at position 166-173, and the miR-145-5p MRE at 298-305 was performed. No significant increase in luciferase by TSB4 or TSB6 was observed from plasmids carrying mutated MREs (Supplementary Fig. 2). Sequence alignment of human and murine CFTR mRNA transcripts, indicates that MREs for TSB4 and TSB6 are not conserved in mice (data not shown).

TSB4 and TSB6 enhance CFTR channel function in CF BECs

We assessed the effect of TSB4 and TSB6 on CFTR function using two established methods. The chloride-sensitive dye MQAE is quenched by intracellular Cl^- ions ($[Cl^-]_i$), therefore increasing fluorescence corresponds to decreasing $[Cl^-]_i$ and improvement of CFTR ion channel activity. After transfection with TSB4 or TSB6 in CFBE41o$^-$ cells, fluorescence significant increased over time (2.7-fold, P=0.0001 and 1.4-fold, P=0.048, compared to NC TSB) (Figure 4A).

These results were validated with the YFP-based CFTR functional assay. YFP fluorescence is quenched by intracellular I^-, therefore decreased fluorescence after applying iodide corresponds to higher influx of I^- and

hence to enhanced CFTR anion channel activity. After co-transfection of the YFP plasmid with TSB4 or TSB6, significant decreases in fluorescence (P=0.0001 for both) were evident both in CFBE41o$^-$ (-18% and -31% when compared to NC TSB) and Cufi-1 (-35% and -70%) cells over time (Figure 4B,C). Taken together, these data indicate that the inhibition of CFTR-specific miRNAs can improve CFTR anion channel activity.

We also tested CFTR activity in a 3D organoid model of lung-specific CFTR function based on forskolin-0induced swelling (FIS) of bronchospheres generated from p.Phe508del/p.Phe508del and syngeneic gene-corrected (p.Phe508del/wild type) iPSCs. miR-145-5p and miR-223-3p were expressed in the CF organoids, and increased in the gene-corrected bronchospheres(Supplementary Fig. 3A,B). Although robust FIS was observed in p.Phe508del/p.Phe508del bronchospheres in response to CFTR modulators (data not shown) there was no immediately observable response to either TSB4 or TSB6 likely due to low transfection efficiency in whole organoids.

TSB4 and TSB6 enhance CFTR modulators effects on CFTR activity in CF BECs

miR-145-5p levels are elevated in CF BALF-derived exosomes,[4] and *Pseudomonas*-conditioned medium or IL-1β can increase expression of miR-145 and/or miR-223 in CFBE41o$^-$ cells,[13] thereby likely decreasing CFTR expression in the inflamed CF lung milieu. Supplementary Fig. 4 shows that CF BALF induces a similar effect by significantly increasing miR-145-5p and miR-223-3p expression in CFBE41o$^-$ and Cufi-1 cells. Thus adjunct therapeutic targeting of the miR-145-5p and miR-223-3p binding sites in the *CFTR* 3'UTR with existing CF modulators could hold merit.

CF BECs were transfected with TSBs and treated with Ivacaftor/Lumacaftor or Ivacaftor/Tezacaftor or DMSO control and YFP fluorescence was assessed. Transfection with TSB4 or TSB6 enhanced the CFTR modulator effects in both CFBE41o$^-$ and Cufi-1 cells (Figure 5). Ivacaftor/Lumacaftor or Ivacaftor/Tezacaftor had no effect on miR-145-5p or miR-223-3p levels in CFBE41o$^-$ or Cufi-1 cells (Supplementary Fig. 5).

Respirable PLGA nanoparticles encapsulating TSB4 and TSB6 increase CFTR in primary CF BECs

PLGA nanoparticles encapsulating TSB4 and TSB6 were formulated. High Content Screening (HCS) confocal images demonstrate cellular uptake and a primarily cytosolic distribution of rhodamine-conjugated TSB4- or TSB6-PLGA nanoparticles by CFBE41o- cells (Figure 6A). Both particles show similar uptake with an average number of spots/cell of 110.2±15.3 for TSB4 and 99.3±14.2 for TSB6. By comparison, untransfected cells

have 16.1±1.4 spots/cell. The PLGA-TSB nanoparticles were non-toxic to CFBE41o- cells and did not induce proinflammatory IL-6 or IL-8 responses (Figure 6B,C).

Ideally such a therapeutic would be aerosolised to the lung. Previously we described the biophysical characteristics of these PLGA-TSB nanoparticles.[18] Here their aerosol characteristics were assessed using the Aerogen Solo nebuliser. They showed no significant differences in their droplet sizes (Supplementary Table 2). The volume median diameter was approximately 4.4 microns for both, and so can be considered a highly respirable aerosol. Nor was there a difference of note in the aerosol output rates (0.51 and 0.48 ml/min). Given the standard 2.5 or 3ml dose volume for inhaled medications this equates to a delivery time of approximately 5 to 6 minutes for both formulations.

Finally a proof-of-principle study demonstrated that PLGA-TSB4 and PLGA-TSB6 could increase CFTR in primary CF BECs (20 and 62%) and that fluorescent versions of the PLGA-TSB nanoparticles transfect well into the same cells (Figure 7A,B,D). Unencapsulated TSB4 and TSB6 also increased CFTR protein expression in primary CF BECs (47 and 61%) (Figure 7C,D).

DISCUSSION

These studies show that CFTR-specific target site blockers can modulate Phe508del CFTR in CF BECs to enhance its expression and anion permeability. miR-145-5p and miR-223-3p showed enhanced expression in Phe508 homozygous CF BEC lines and BECs from children and adults with CF. These miRNAs were also expressed in CF and CFTR gene-corrected iPSC-derived CF lung organoids. TSBs precisely targeting specific individual binding sites of these miRNAs in the *CFTR* 3'UTR were effective at enhancing CFTR protein levels in two Phe508del homozygous BEC lines. Delivery of the TSBs encapsulated in PLGA nanoparticles also increased CFTR expression in primary CF BECs, providing a proof-of-principle for aerosol delivery of TSBs for inhalation therapy in CF lung. We concentrated our studies on human CF models because murine CFTR is not regulated by the same miRNAs as human CFTR.

Previously TSBs targeting unspecified miR-101 and miR-145 sites in the CFTR 3'UTR demonstrated increased CFTR expression and function in CF nasal epithelial cells.[19] However, there are five and eight sites each for miR-101-3p and miR-145-5p in the CFTR 3'UTR. Therefore in this work we took into account not only these 13 binding sites but all other predicted binding sites for the lead miRNAs that have been demonstrated to regulate CFTR. In total 31 individual MREs were considered, and TSBs were designed to the nine sites predicted to be most functional. Ultimately, independently inhibiting two specific MREs was found to

be most effective; the miR-145-5p site located at 298-305 and miR-223-3p at 166-173. There was no additive effect of combining TSB4 and TSB6 (data not shown) possibly due to steric hindrance between the closely located MREs.

The TSBs work by blocking the binding of miR-145-5p and miR-223-3p to specific sites in the CFTR 3'UTR. The increased anion flux in CF BECs observed following individual TSB treatment most likely arises from an increased number of functional Phe508del CFTR channels in the plasma membrane, rather than changes in channel selectivity or gating.

PLGA is a synthetic polymer approved by the US FDA and European Medicine Agency in various drug delivery systems in humans. It is widely used due to its inherent biocompatibility, low toxicity and immunogenicity, and biodegradability.[18] *In vivo*, PLGA is removed by the citric acid cycle. PLGA drug carriers can achieve sustained cytoplasmic delivery via rapid escape from endolysosomes. Previously we reported a comprehensive biophysical investigation of the PLGA-TSB4 and PLGA-TSB6 nanoparticles[18] (therein termed LNA1 and 2, respectively). Size distribution, polydispersity index and zeta potential revealed the nanoparticle diameters were ~200 nm and transmission electronic microscopy confirmed they had a monodisperse particle size distribution. The surface charge was neutral to slightly negative, and a high amount of each TSB was encapsulated by the PLGA. When nebulized, there were no differences in particle size versus prior to nebulization. The work presented here builds on that study. The data demonstrate functional properties of the PLGA-TSB nanoparticles in primary CF BECs, as well as desirable volumetric median diameter and fine particle fraction values that are indicative of highly respirable aerosols with nebulizer output rates that would ensure reasonable treatment times. This is a key consideration in the CF patient population where the daily burden of aerosol and other therapies is already high.

Here we also provide the first report of a synergistic effect of specific miRNA binding site inhibition in combination with CFTR correctors, to enhance anion flux through Phe508del-CFTR. CF BECs display increased functionally active Phe508del-CFTR when treated with a combination of TSBs and CFTR modulators. These findings indicate a therapeutic value in selectively inhibiting the activity of specific miRNAs in CF BECs to potentiate the effectiveness of CFTR modulators. This is important because, not only are miRNAs that regulate CFTR increased basally in CF BECs, but the proinflammatory CF lung milieu increases expression of CFTR-specific miRNAs, as we have shown here and elsewhere.[13] This has also been demonstrated for miR-145-5p in CF BALF exosomes, where it was first reported that increased miR-145-5p nullifies CFTR correction by Ivacaftor/Lumacaftor.[4]

Traditional CF therapies target the loss of function of CFTR. Pharmaceutical modulators can restore function to mutant CFTR however, optimal therapy and effective personalised medicine may require combinations of CFTR correctors with adjunct therapies. Here we found a potentiating effect of two TSBs on CFTR modulators to enhance Phe508del-CFTR function. CF BECs transfected with TSBs potentiated the effects of Ivacaftor/Lumacaftor or Ivacaftor/Tezacaftor on anion permeability of Phe508del-CFTR. Our findings of an enhanced anion flux through Phe508del-CFTR when the CFTR modulators were applied after transfection with TSB4 or TSB6 indicate that miR-223-3p and miR-145-5p, respectively, exert an inhibitory effect on CFTR function. When this inhibition is relieved with TSB transfection, the efficacy of Ivacaftor/Lumacaftor on CFTR function was enhanced up to five-fold. The ability of TSBs to enhance up to three-fold the corrector effects of Ivacaftor/Tezacaftor on Phe508del-CFTR function further strengthens the relevance of inhibition of specific MREs as adjunct therapy in treating CF lung disease.

There are limitations to this study. It was not possible to perform all assays in all of the models used, and functional analyses other than CFTR were beyond the scope of the current work. The lack of an observable effect of the TSBs in bronchospheres due to poor transfection was disappointing, and is a challenge that faces the entire field in the development of anti-sense oligonucleotide delivery using *in vitro* organoid models of disease.[20-22] To our knowledge there is no description of locked nucleic acid delivery to organoids in the literature and new methods will need to be developed to study their effects. Mucus-penetrating studies were also beyond the scope of this work however such studies will be important in the next steps of assessing this drug-device combination.[23]

Overall the findings suggest that alone or in combination with CFTR modulators, aerosolized CFTR-targeting TSBs encapsulated in PLGA nanoparticles could represent a promising therapeutic strategy for the treatment for CFTR dysfunction in CF bronchial epithelium. In conclusion, the precise and selective inhibition of specific miRNAs binding to the CFTR 3'UTR in CF BECs may offer an alternative or adjunct therapy to improve airway CFTR function in individuals homozygous for the p.Phe508del CFTR mutation.

MATERIAL AND METHODS

Additional details are provided in the Supplementary file.

Cells, patient samples and treatments

Non-CF (16HBE14o$^-$, Nuli-1) and CF (CFBE41o$^-$, Cufi-1) human BECs, CFBE41o- stably transduced with WT-CFTR or Phe508del-CFTR, primary human BECs isolated from the proximal airways of six non-CF (five males, mean age 41.6±8.0 years) and six CF adults (two males, mean age 29.3±1.1) or purchased commercially, BECs isolated from six non-CF and six CF children (all male, mean age CF: 3±2.5 years, non-CF: 3.3±1.5 years), and CF and syngeneic gene-corrected (p.Phe508del/wild type) bronchospheres generated from induced pluripotent stem cells were studied. All CF cells/samples were p.Phe508del/p.Phe508del. Where indicated cells were treated with CFTR modulators (5 μM each) alone or in combination with TSBs or 1% CF bronchoalveolar lavage fluid (BALF). Ethics committee approval and informed consent were granted for all clinical samples.

miRNA quantification

TaqMan MicroRNA Reverse Transcription Kit and pre-designed TaqMan MicroRNA assays (ThermoFisher Scientific) were used for individual miRNA quantification on the LC480 LightCycler (Roche). Profiling of CF and non-CF paediatric samples was performed with TaqMan OpenArray Human MicroRNA Panels on the QuantStudio 12K Flex system (ThermoFisher Scientific), GEO GSE128861. Following library generation RNA sequencing of CFBE41o- stably transduced with WT-CFTR or Phe508del-CFTR was performed on the Illumina NextSeq 500,[24-26] GEO GSE128912.

Target site blockers

TSBs were designed (Exiqon) to compete with miR-101-3p, miR-145-5p, miR-223p, miR-494-3p and miR-509-3p binding to specific sites in the CFTR 3'UTR (Supplementary Table 1).

Luciferase assay

CFBE41o$^-$ cells were co-transfected with TSBs and wildtype[27] or mutant CFTR 3'UTR luciferase reporter plasmids. Luciferase activity was assessed by Dual-Luciferase Reporter Assay (Promega).

CFTR assays

CFTR and β-actin were visualised in total protein extracts by western blot. CFTR activity in cell lines was measured using N-(ethoxycarbonylmethyl)-6-methoxyquinolinium bromide (MQAE)[13] and yellow fluorescent protein (YFP)-H148Q/I152L.[28,29] Forskolin-induced swelling was measured in CF bronchospheres.[30]

PLGA nanoparticles

PLGA-TSB nanoparticles were formulated[18] and MTT assay, IL-6 and IL-8 ELISA were performed as before.[31] Nanoparticles were analysed by high content screening.[32] Following nebulization (Aerogen Solo) aerosol characteristics were measured using laser diffraction.[33]

Statistical analysis

Analyses were performed using GraphPad PRISM 7.0. Results are expressed as mean±SEM and compared as indicated. Differences were considered statistically significant when $P \leq 0.05$.

ACCESSION NUMBERS

Profiling data from n=6 paediatric CF and non-CF BECs have been deposited with the Gene Expression Omnibus repository under accession number GEO GSE128861. RNA sequencing data from ALI culture of CFBE41o– cells stably transfected with Phe508del versus wild-type CFTR have been deposited with the Gene Expression Omnibus repository under accession number GEO GSE128912.

SUPPLEMENTARY DATA

Supplementary Data are available at Molecular Therapy online.

ACKNOWLEDGEMENT

Thank you to Andrew Berical and Rhiannon Werder in Center for Regenerative Medicine, Boston University and Boston Medical Center and The Pulmonary Center and Department of Medicine, Boston University School of Medicine, and Ruby Wang from Boston Children's Hospital, Harvard Medical School, Boston, Massachusetts, USA for technical assistance. Thank you to Dr Nicoletta Pedemonte from Gaslini Institute (Genova) who kindly donated the plasmid encoding YFP-H148Q/I152L protein. This work was supported by Cystic Fibrosis Foundation Therapeutics [GREENE15XXO to C.M.G.]; National Children's Research Centre [C/13/1 to C.M.G.], The National Institutes of Health [R01HL144539 to A.S.U.]; Cystic Fibrosis Foundation [SWIATE18G0 to A.S.U.], Horizon2020 MSCA-IF [award 707771 GENDER-CF to A.M.G.], and the Irish Research Council [GOIPG/2015/2393 to R.G.]. The authors have no relevant conflicts of interest to declare other than the receipt of funding form the named agencies to carry out the current work.

Author Contributions

C.D.S.: study design, data collection, data analysis, data interpretation, figures, writing. E.F.F, I.O., N.M. and M.B.C: data collection, data analysis, data interpretation, figures. R.G.: data collection, data analysis, data interpretation, figures, funding acquisition. S.V.: data collection, data analysis, data interpretation. A.G.: data collection, data analysis, figures, funding acquisition. K.H. and F.H.: data collection, data analysis, data interpretation, figures, writing. F.M.: data analysis, data interpretation, figures. R.R., D.H. and J.S.: data collection, data analysis. B.J.H.: writing, funding acquisition. B.L. and S.A.C: data collection, funding acquisition. P.McN.: data collection, writing, funding acquisition. R.MacL. and A.S.U.: data collection, data analysis, data interpretation, figures, writing, funding acquisition. C.M.G.: Conceptualization, study design, data analysis, data interpretation, figures,writing, funding acquisition.

REFERENCES

1. Rommens, J.M., Iannuzzi, M.C., Kerem, B., Drumm, M.L., Melmer, G., Dean, M., Rozmahel, R., Cole, J.L., Kennedy, D., Hidaka, N., et al. (1989) Identification of the cystic fibrosis gene: chromosome walking and jumping. Science, *245*, 1059–65.

2. Riordan, J.R., Rommens, J.M., Kerem, B., Alon, N., Rozmahel, R., Grzelczak, Z., Zielenski, J., Lok, S., Plavsic, N., Chou, J.L., et al. (1989) Identification of the cystic fibrosis gene: cloning and characterization of complementary DNA. Science, *245*, 1066–73.

3. Glasgow, A.M.A., De Santi, C., Greene, C.M. (2018) Non-coding RNA in cystic fibrosis. Biochem. Soc. Trans., *46*, 619–630.

4. Lutful Kabir, F., Ambalavanan, N., Liu, G., Li, P., Solomon, G.M., Lal, C.V., Mazur, M., Halloran, B., Szul, T., Gerthoffer, W.T., et al. (2018) MicroRNA-145 Antagonism Reverses TGF-β Inhibition of F508del CFTR Correction in Airway Epithelia. Am J. Respir. Crit. Care, *197*, 632–643.

5. Fabbri, E., Tamanini, A., Jakova, T., Gasparello, J., Manicardi, A., Corradini, R., Sabbioni, G., Finotti, A., Borgatti, M., Lampronti, I., et al. (2017) A Peptide Nucleic Acid against MicroRNA miR-145-5p Enhances the Expression of the Cystic Fibrosis Transmembrane Conductance Regulator (CFTR) in Calu-3 Cells. Molecules, *23*, E71.

6. Amato, F., Tomaiuolo, R., Nici, F., Borbone, N., Elce, A., Catalanotti, B., D'Errico, S., Morgillo, C.M., De Rosa, G., Mayol, L., et al. (2014) Exploitation of a very small peptide nucleic acid as a new inhibitor of miR-509-3p involved in the regulation of cystic fibrosis disease-gene expression. Biomed. Res. Int., 610718.

7. Finotti, A., Gasparello, J., Fabbri, E., Tamanini, A., Corradini, R., Dechecchi, M.C., Cabrini, G., Gambari, R. (2019) Enhancing the Expression of CFTR Using Antisense Molecules Against MicroRNA miR-145-5p. Am. J. Respir. Crit. Care. Med., *199*, 1443-1444.

8. Sonneville, F., Ruffin, M., Coraux, C., Rousselet, N., Le Rouzic, P., Blouquit-Laye, S., Corvol, H., Tabary, O. (2017) MicroRNA-9 downregulates the ANO1 chloride channel and contributes to cystic fibrosis lung pathology. Nat. Commun., *8*, 710.

9. Van Goor, F., Hadida, S., Grootenhuis, P.D., Burton, B., Cao, D., Neuberger, T., Turnbull, A., Singh, A., Joubran, J., Hazlewood, A., et al. (2009) Rescue of CF airway epithelial cell function in vitro by a CFTR potentiator, VX-770. Proc. Natl. Acad. Sci. U S A, *106*, 18825–30.

10. Van Goor, F., Hadida, S., Grootenhuis, P.D., Burton, B., Stack, J.H., Straley, K.S., Decker, C.J., Miller, M., McCartney, J., Olson, E.R., et al. (2011) Correction of the F508del-CFTR protein processing defect in vitro by the investigational drug VX-809. Proc. Natl. Acad. Sci. U S A, *108*, 18843–8.

11. Elborn, J.S., Ramsey, B.W., Boyle, M.P., Konstan, M.W., Huang, X., Marigowda, G., Waltz, D., Wainwright, C.E., VX-809 TRAFFIC and TRANSPORT study groups. (2016) Efficacy and safety of lumacaftor/ivacaftor combination therapy in patients with cystic fibrosis homozygous for Phe508del CFTR by pulmonary function subgroup: a pooled analysis. Lancet Respir. Med., *4*, 617–626.

12. Rowe, S.M., Daines, C., Ringshausen, F.C., Kerem, E., Wilson, J., Tullis, E., Nair, N., Simard, C., Han, L., Ingenito, E.P., et al. (2017) Tezacaftor-Ivacaftor in Residual-Function Heterozygotes with Cystic Fibrosis. N. Engl. J. Med. *377*, 2024–2035.

13. Oglesby, I.K., Chotirmall, S.H., McElvaney, N.G., Greene, C.M. (2013) Regulation of cystic fibrosis transmembrane conductance regulator by microRNA-145, -223, and -494 is altered in ΔF508 cystic fibrosis airway epithelium. J. Immunol., *190*, 3354–62.

14. Dugernier, J., Hesse, M., Vanbever, R., Depoortere, V., Roeseler, J., Michotte, J.B., Laterre, P.F., Jamar, F., Reychler, G. (2017) SPECT-CT Comparison of Lung Deposition using a System combining a Vibrating-mesh Nebulizer with a Valved Holding Chamber and a Conventional Jet Nebulizer: a Randomized Cross-over Study. Pharm. Res. *34*, 290–300.

15. Altenburg, A.F., van de Sandt, C.E., Li, B.W.S, MacLoughlin, R.J., Fouchier, R.A.M., van Amerongen, G., Volz, A., Hendriks, R.W., de Swart, R.L., Sutter G, et al. (2017) Modified Vaccinia Virus Ankara Preferentially Targets Antigen Presenting Cells In Vitro, Ex Vivo and In Vivo. Sci. Rep., *7*, 8580.

16. Oglesby, I.K., Bray, I.M., Chotirmall, S.H., Stallings, R.L., O'Neill, S.J., McElvaney, N.G., Greene, C.M. (2010) miR-126 is downregulated in cystic fibrosis airway epithelial cells and regulates TOM1 expression. J. Immunol., *184*, 17029.

17. van Meegen, M.A., Terheggen, S.W., Koymans, K.J., Vijftigschild, L.A., Dekkers, J.F., van der Ent, C.K., Beekman, J.M. (2013) CFTR-mutation specific applications of CFTR-directed monoclonal antibodies. J. Cyst. Fibros.,*12*, 487–96.

18. Fernández Fernández, E., Santos-Carballal, B., de Santi, C., Ramsey, J.M., MacLoughlin, R., Cryan, S.A., Greene, C.M. (2018) Biopolymer-Based Nanoparticles for Cystic Fibrosis Lung Gene Therapy Studies. Materials (Basel), *11*, E122.

19. Viart, V., Bergougnoux, A., Bonini, J., Varilh, J., Chiron, R., Tabary, O., Molinari, N., Claustres, M., Taulan-Cadars, M. (2015) Transcription factors and miRNAs that regulate fetal to adult CFTR expression change are new targets for cystic fibrosis. Eur. Respir. J., *45*, 116–28.

20. Bhise, N.S., Gray, R.S., Sunshine, J.C., Htet, S., Ewald, A.J., Green, J.J. (2010) The relationship between terminal functionalization and molecular weight of a gene delivery polymer and transfection efficacy in mammary epithelial 2-D cultures and 3-D organotypic cultures. Biomaterials, *31*, 8088–96.

21. Mellor, H.R., Davies, L.A., Caspar, H., Pringle, C.R., Hyde, S.C., Gill, D.R., Callaghan, R. (2006) Optimising non-viral gene delivery in a tumour spheroid model. J. Gene Med., *8*, 1160–70.

22. Juliano RL. (2016) The delivery of therapeutic oligonucleotides. Nucleic Acids Res., *44*, 6518–48.

23. Pacheco, D.P., Butnarasu, C.S., Briatico Vangosa, F., Pastorino, L., Visai, L., Visentin, S., Petrini, P. (2019) Disassembling the complexity of mucus barriers to develop a fast screening tool for early drug discovery. J. Mater. Chem. B., *7*, 4940-52.

24. Swiatecka-Urban, A., Brown, A., Moreau-Marquis, S., Renuka, J., Coutermarsh, B., Barnaby, R., Karlson, K.H., Flotte, T.R., Fukuda, M., Langford, G.M., Stanton, B.A. (2005) The short apical membrane half-life of rescued deltaF508-CFTR results from accelerated endocytosis delta F508del-CFTR in polarized human airway epithelial cells. J. Biol. Chem., *280*, 36762–72.

25. Snodgrass, S.M., Cihil, K.M., Cornuet, P.K., Myerburg, M.M., Swiatecka-Urban, A. (2013) TGF-beta1 Inhibits CFTR Biogenesis and Prevents Functional Rescue of DeltaF508-CFTR in Primary Differentiated Human Bronchial Epithelial Cells. PLoS. One, *8*, e63167.
26. Barberan-Soler, S., Vo, J.M., Hogans, R.E., Dallas, A., Johnston, B.H, Kazakov, S.A. (2018) Decreasing miRNA sequencing bias using a single adapter and circularization approach. Genome Biol., *19*, 105.
27. De Santi, C., Gadi, S., Swiatecka-Urban, A., Greene, C.M. (2018) Identification of a novel functional miR-143-5p recognition element in the Cystic Fibrosis Transmembrane Conductance Regulator 3'UTR. AIMS Genetics, *5*, 53–62.
28. Galietta, L.V., Jayaraman, S., Verkman, A.S. (2001) Cell-based assay for high-throughput quantitative screening of CFTR chloride transport agonists. Am. J. Physiol. Cell. Physiol., *281*, C1734-42.
29. Caputo, A., Hinzpeter, A., Caci, E., Pedemonte, N., Arous, N., Di Duca, M., Zegarra-Moran, O., Fanen, P., Galietta, L.J. (2009) Mutation-specific potency and efficacy of cystic fibrosis transmembrane conductance regulator chloride channel potentiators. J. Pharmacol. Exp. Ther. *330*, 783–91.
30. McCauley, K.B., Hawkins, F., Serra, M., Thomas, D.C., Jacob, A., Kotton, D.N. (2017) Efficient Derivation of Functional Human Airway Epithelium from Pluripotent Stem Cells via Temporal Regulation of Wnt Signaling. Cell. Stem. Cell., *20*, 844–857.
31. Vencken, S., Foged, C., Ramsey, J., Sweeney, L., Cryan, S.A., MacLoughlin, R., Greene, C.M. (2019) Nebulised Lipid-Polymer Hybrid Nanoparticles for the Delivery of a Therapeutic Anti-inflammatory microRNA to Bronchial Epithelial Cells. Eur. Respir. J. Open. Res., *5*, 2.
32. Walsh, D.P., Murphy, R.D., Panarella, A., Raftery, R.M., Cavanagh, B., Simpson, J.C., O'Brien, F.J., Heise, A., Cryan, S.A. (2018) Bioinspired Star-Shaped Poly(l-lysine) Polypeptides: Efficient Polymeric Nanocarriers for the Delivery of DNA to Mesenchymal Stem Cells. Mol. Pharm. *15*, 1878–1891.
33. Hibbitts, A., O'Mahony, A.M., Forde, E., Nolan, L., Ogier, J., Desgranges, S., Darcy, R., MacLoughlin, R., O'Driscoll, C.M., Cryan, S.A. (2014) Early-stage development of novel cyclodextrin-siRNA nanocomplexes allows for successful postnebulization transfection of bronchial epithelial cells. J. Aerosol. Med. Pulm. Drug. Deliv., *27*, 466–77.

FIGURES LEGENDS

Figure 1. miRNA levels in CF and non-CF cell line and primary bronchial epithelial cells. Relative expression levels, shown as fold change (%), of miRNAs were determined by qRT-PCR using individual Taqman assays and normalised to U6snRNA in (A) CFBE410- vs. 16HBE14o-, (B) Cufi-1 vs. Nuli-1 or (C) adult CF vs. non CF primary cells (n=6 in triplicate for each cell line) . Data are presented as mean ± SEM and were compared by one-way ANOVA (Dunnett's multiple comparisons test *P<0.05,**P<0.01, ****P<0.0001). (D) Volcano plot generated from miRNA-Seq showing differential expression of miRNAs in CFBE41o- ALI-cultured cells stably transfected with Phe508del (CF), compared to WT (Non-CF) CFTR. miRNAs conserved in mammals (black, TargetScanHuman Release 7.2), non-conserved miRNAs (grey). P <0.05 corresponding to –Log10 >1.3. N=6/group from different cultures. Dashed line indicates P=0.05.

Figure 2. Target Site Blocker design and screening and selection of CFTR-specific TSBs. (A) Visual map of the in silico predictions of miRNA responsive elements (MREs) of the five lead miRNAs (i.e. miR-101-3p, miR-145-5p, miR-223-3p, miR-494-3p and miR-509-3p) within the CFTR 3'UTR. (B) Table showing the prediction of the target sites of the lead miRNAs on CFTR 3'UTR according to PITA algorithm. ΔΔG is ΔG(duplex)–ΔG(open) where ΔG(duplex) is the hybridization energy of the miRNA to the binding site and ΔG(open) is the energy required to open the local RNA secondary structure around the binding site. The more negative the ΔΔG the stronger the expected binding of a miRNA to that site. (C) CFTR 3'UTR luciferase activity reported as relative light units (RLU) in % in CFBE41o- cells (n=3 in triplicate). Data are presented as mean ± SEM and were compared by one-way ANOVA (Dunnett's multiple comparisons test *P<0.05,**P<0.01, ****P<0.0001). Samples transfected with non-targeting control (NC) TSB are reported as reference and set at 0%.

Figure 3. Effect of CFTR-specific TSBs on CFTR protein expression. Western blot of endogenous CFTR protein following TSBs transfection in (A) CFBE41o- (n=5) and (B) Cufi-1 (n=3) CF bronchial epithelial cells. Quantification after internal normalisation with β-actin is displayed together with a representative image. In both CF cell lines, CFTR migrated with a band at ~130 kDa that corresponds at the immature (i.e. unglycosylated band A) form which was used for quantification. In Cufi-1, CFTR band B (core glycosylated band B) was also visible in some experiments. Data are presented as mean ± SEM and were compared by

one-way ANOVA (Dunnett's multiple comparisons test), **P < 0.01. Samples transfected with non-targeting control (NC) TSB are reported as reference and set at 100%.

Figure 4. CFTR functional assays in CF bronchial epithelial cells. CFTR activity 48 h post transfection with a non-targeting control (NC) TSB, TSB4 or TSB6 was assessed with the chloride-sensitive dye MQAE in (A) CFBE41o- cells and the halide-sensitive YFP in (B) CFBE41o- and (C) Cufi-1 cells. All experiments were performed after stimulation of CFTR with 20 μM of forskolin (FSK) (n>3 per cell line, in triplicate). Data are presented as background-corrected fluorescence values normalised for the initial fluorescence (i.e. baseline fluorescence for MAQE assay and fluorescence measured before addition of I- for YFP assay) over time and compared by two-way ANOVA (Dunnett's multiple comparisons test *P<0.05, ****P<0.0001).

Figure 5. YFP assay in CF bronchial epithelial cells transfected with TSBs in combination with CFTR modulators. (A) CFBE41o- and (B) Cufi-1 cells were transfected with a non-targeting control (NC) TSB, TSB4 or TSB6 then immediately treated with DMSO or ivacaftor/lumacaftor (black) or ivacaftor/tezacaftor (grey) for 48h. All experiments were performed after stimulation of CFTR with 20 μM of forskolin (FSK), (n>3 per cell line, in triplicate). Data are presented as average of the background-corrected fluorescence values normalised for the initial fluorescence (i.e. fluorescence measured before addition of I-) and compared by two-way ANOVA (Dunnett's multiple comparisons test *P<0.05, **P<0.01, ***P<0.001, ****P<0.0001).

Figure 6. Delivery and toxicity of PLGA-TSBs in CFBE41o- cells. (A) Representative images (Scale= 20 μm) and quantitation of high content screening of rhodamine-conjugated PLGA-TSB4 or -TSB6 nanoparticles (red) into CFBE41o- cells (n=12-24 wells each). Cell nuclei are stained blue. An example of the nanoparticles being detected and segmented within the population of cells using 'Find Spots' is shown in the bottom right of each image. Effect of PLGA-TSBs on (B) viability at 48 h (TX, Triton X-100 positive control), and (C) IL-6 and IL-8 cytokine release from CFBE41o- cells after 24 h, n=3 (CF BALF 1% and LPS 10 μg/ml, positive controls). Data are presented as mean ± SEM, *P<0.05 and ****P<0.0001.

Figure 7. Effect of TSBs or PLGA-TSBs on CFTR protein expression in primary CF cells. Western blot of CFTR and β-actin protein 72 h following (A) PLGA-TSB (N:P ratio 10) or (C) TSB transfection into primary CF bronchial epithelial cells. (B) Representative epifluorescence microscopy images of transfection of rhodamine-conjugated PLGA-TSB4 or -TSB6 into primary CF bronchial epithelial cells at 24 hours after transfection. (D)

Quantification of CFTR after internal normalisation with β-actin (n=2). Control samples are reported as reference and set at 100%.

Figure 1

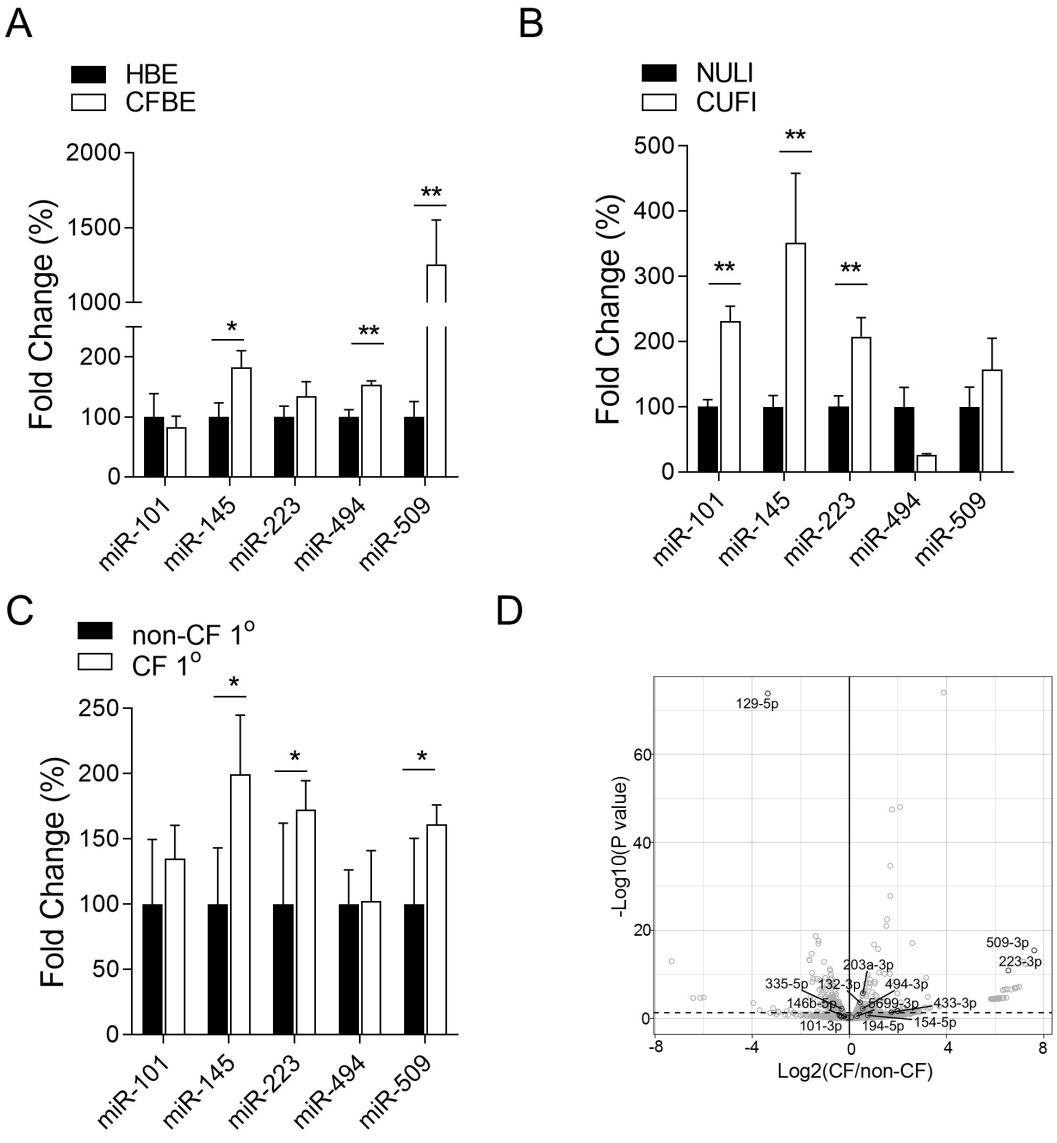
A
HBE
CFBE
Fold Change (%)
2000
1500
1000
200
100
0
*
**
**
miR-101
miR-145
miR-223
miR-494
miR-509
B
NULI
CUFI
Fold Change (%)
500
400
300
200
100
0
**
**
**
miR-101
miR-145
miR-223
miR-494
miR-509
C
non-CF 1°
CF 1°
Fold Change (%)
250
200
150
100
50
0
*
*
*
miR-101
miR-145
miR-223
miR-494
miR-509
D
-Log10(P value)
60
40
20
0
129-5p
509-3p
223-3p
203a-3p
335-5p
132-3p
494-3p
146b-5p
5699-3p
433-3p
101-3p
194-5p
154-5p
-8
-4
0
4
8
Log2(CF/non-CF)

Figure 2

A Human *CFTR* 3'UTR; 1556 bp

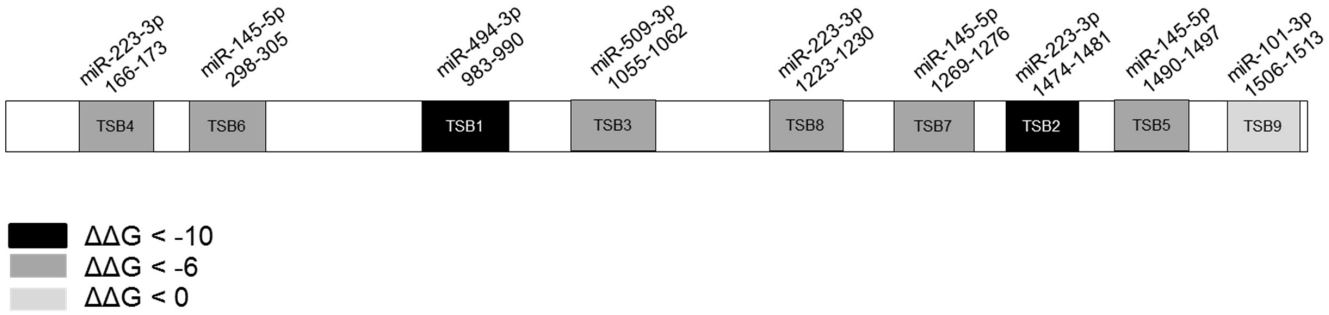

B

TSB	miRNA	Position	ΔΔG
1	494-3p	983	-13.46
2	223-3p	1474	-10.45
3	509-3p	1055	-7.52
4	223-3p	166	-6.78
5	145-5p	1490	-6.63
6	145-5p	298	-6.5
7	145-5p	1269	-6.48
8	223-3p	1223	-6.03
9	101-3p	1506	-2.91

C

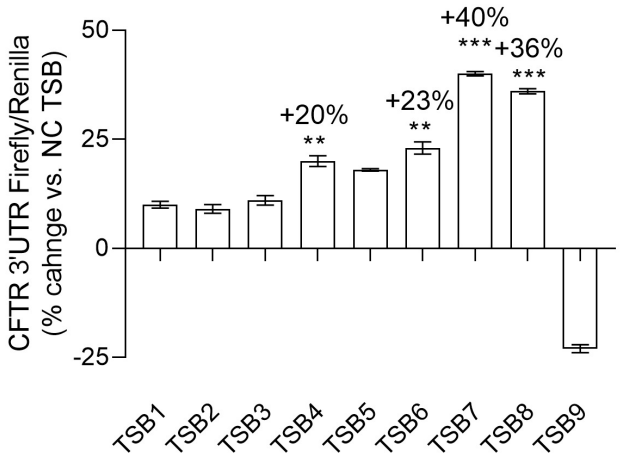

Figure 3

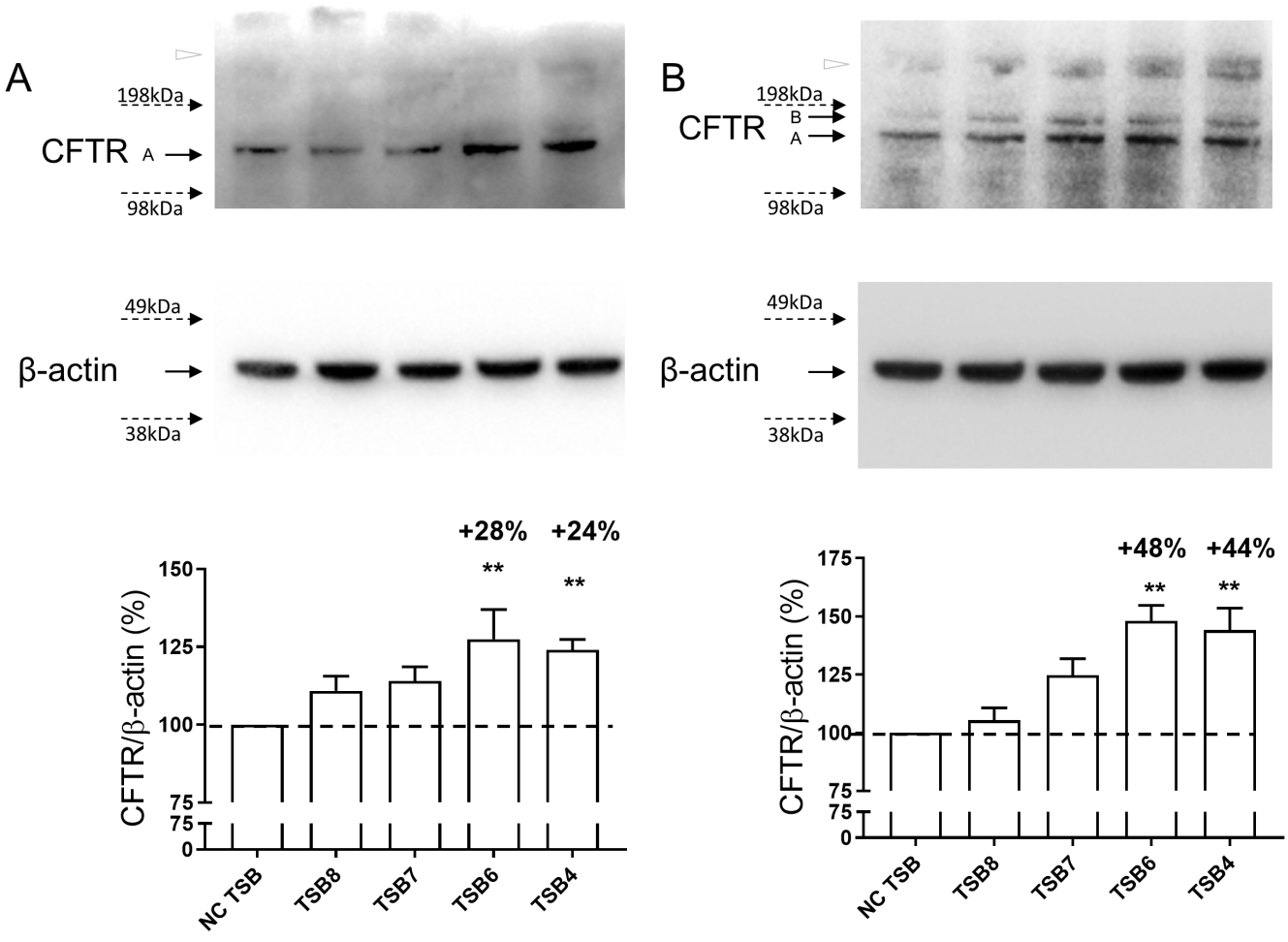
A
198kDa
CFTR A
98kDa
49kDa
β-actin
38kDa
B
198kDa
CFTR B A
98kDa
49kDa
β-actin
38kDa
CFTR/β-actin (%)
+28%
+24%
**
**
NC TSB
TSB8
TSB7
TSB6
TSB4
+48%
+44%

Figure 4

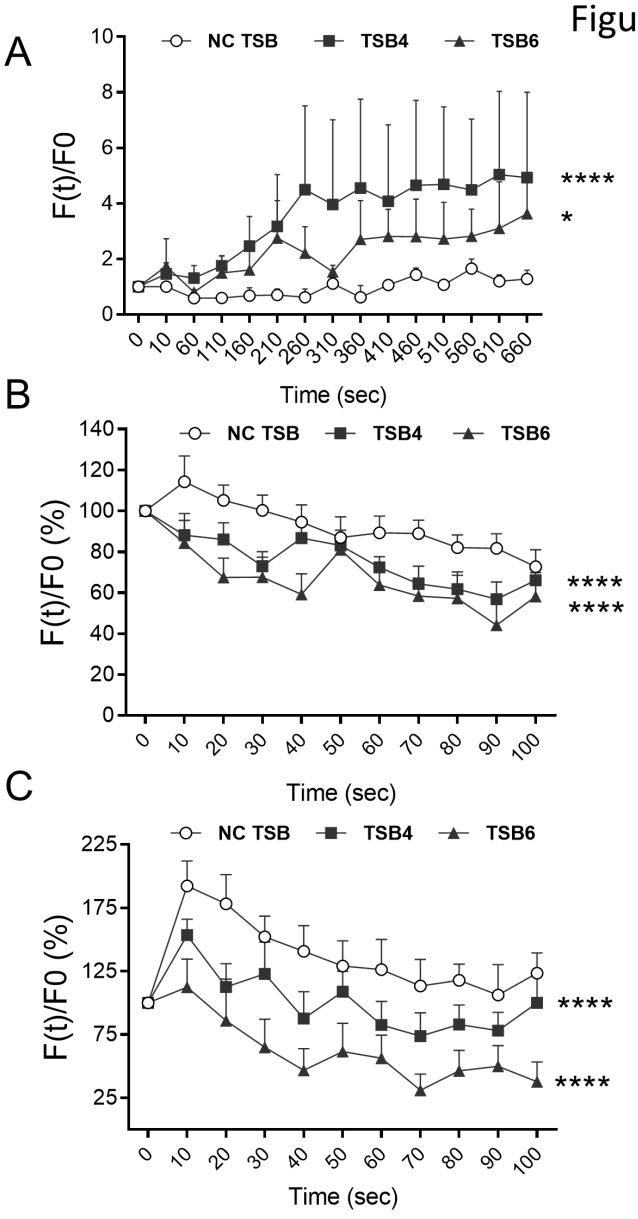
A
NC TSB
TSB4
TSB6
F(t)/F0
Time (sec)
****
*
B
NC TSB
TSB4
TSB6
F(t)/F0 (%)
Time (sec)
****
****
C
NC TSB
TSB4
TSB6
F(t)/F0 (%)
Time (sec)
****
****

Figure 5

A

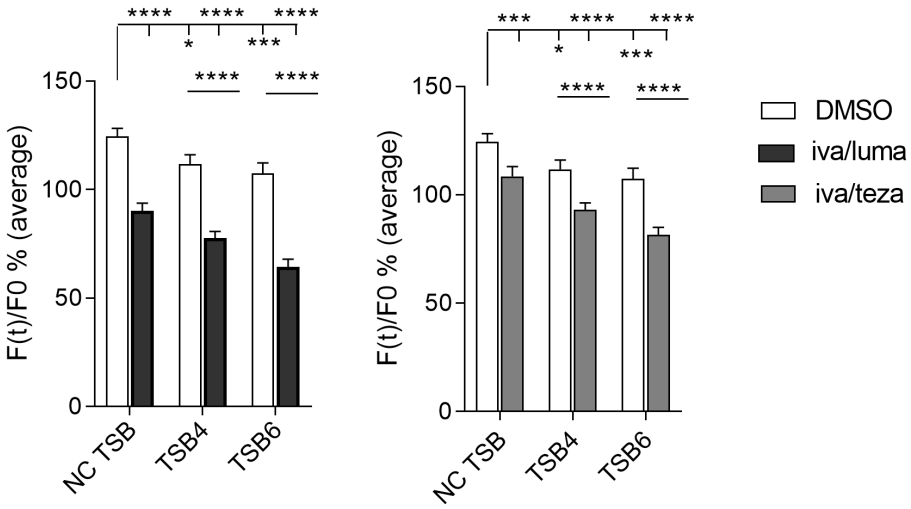
****
****
****
*
***
****
****
150
100
50
0
F(t)/F0 % (average)
NC TSB
TSB4
TSB6
***
****
****
*
***
****
****
DMSO
iva/luma
iva/teza

B

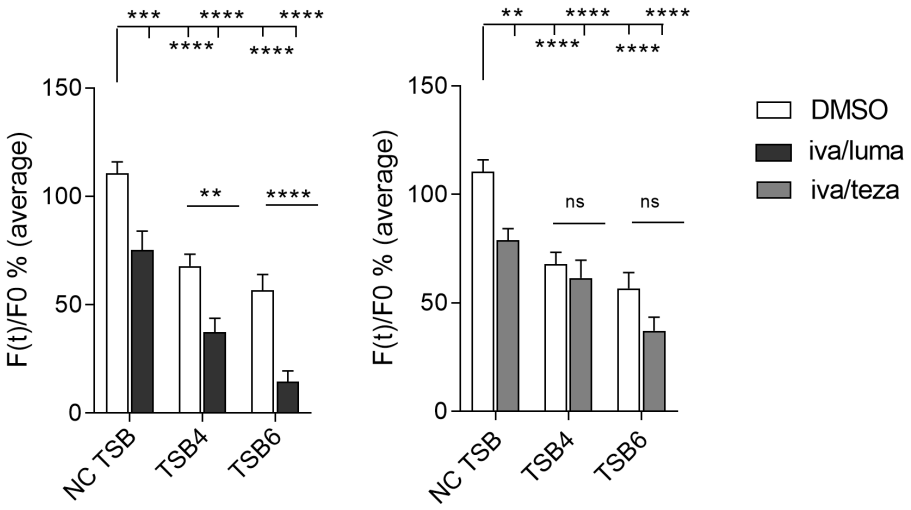
***
****
****
****
****
**
****
150
100
50
0
F(t)/F0 % (average)
NC TSB
TSB4
TSB6
**
****
****
****
****
ns
ns
DMSO
iva/luma
iva/teza

Figure 6

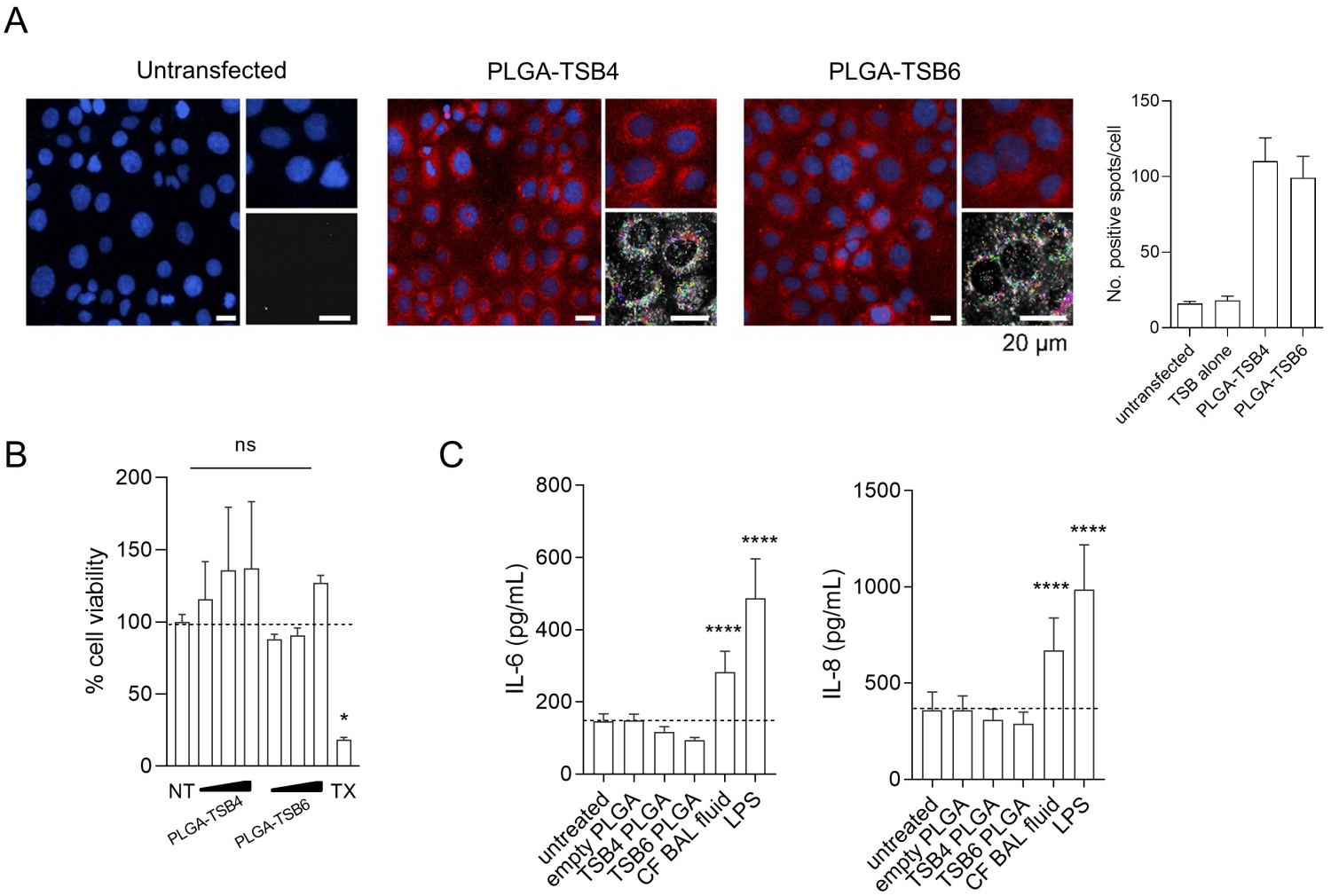
A
Untransfected
PLGA-TSB4
PLGA-TSB6
20 µm
No. positive spots/cell
150
100
50
0
untransfected
TSB alone
PLGA-TSB4
PLGA-TSB6
B
ns
% cell viability
200
150
100
50
0
*
NT
TX
PLGA-TSB4
PLGA-TSB6
C
IL-6 (pg/mL)
800
600
400
200
0
****
****
IL-8 (pg/mL)
1500
1000
500
0
****
****
untreated
empty PLGA
TSB4 PLGA
TSB6 PLGA
CF BAL fluid
LPS

Figure 7

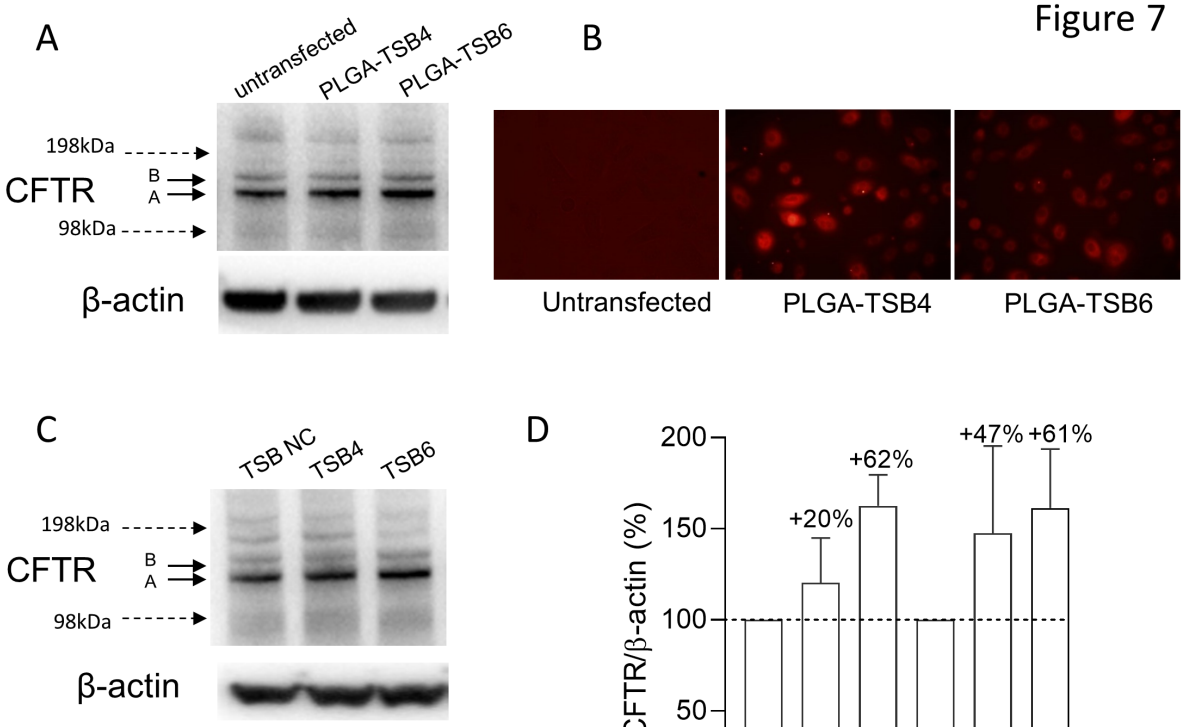
A
untransfected
PLGA-TSB4
PLGA-TSB6
198kDa
CFTR
B
A
98kDa
β-actin
B
Untransfected
PLGA-TSB4
PLGA-TSB6
C
TSB NC
TSB4
TSB6
198kDa
CFTR
B
A
98kDa
β-actin
D
CFTR/β-actin (%)
200
150
100
50
0
+20%
+62%
+47%
+61%
PLGA-NC
PLGA-TSB4
PLGA-TSB6
NC
TSB4
TSB6